Article

Not peer-reviewed version

Impact of Hydrocarbon Emissions from Oil and Gas Deposits on δ13C Variability in Pine Tree Rings

Olga V. Churakova (Sidorova) * , Georgy Batalin , Bulat Gareev , Gazinur Mingazov , Andrey Terekhin , Denis Tishin , Dilyara Kuzina , Danis Nurgaliev

Posted Date: 3 October 2023

doi: 10.20944/preprints202310.0090.v1

Keywords: CO2; CH4; δ13C in wood; tree-ring; Pinus sylvestris; iWUE; ci/ca; temperature; precipitation; evapotranspiration; cloud fraction; Tatarstan Republic; Russia

Article

Impact of Hydrocarbon Emissions from Oil and Gas Deposits on $\delta^{13}C$ Variability in Pine Tree Rings from Tatarstan Republic

Olga V. Churakova (Sidorova) [1,2,3,*], Georgii Batalin [3], Bulat Gareev [3], Gazinur Mingazov [3], Andrey Terekhin [3], Denis Tishin [3], Dilyara Kuzina [3] and Danis Nurgaliev [3]

[1] Siberian Federal University Krasnoyarsk, 660041 Svobodny 79, Russian Federation ochurakova@sfu-kras.ru
[2] Swiss Federal Institute for Forest, Snow and Landscape Research WSL, Zürcherstrasse 111, CH-8903 Birmensdorf, Switzerland
[3] Kazan Federal University, Institute of Geology and Petroleum Technologies, Kremlyovskaya str. 18, Kazan 420008, Russian Federation
* Correspondence: Olga V. Churakova (Sidorova) ochurakova@sfu-kras.ru

Abstract: Human-caused anthropogenic greenhouse emissions impact climate globally. In this pilot study, we aim to reveal influence of hydrocarbon emissions from the giant oil field reservoirs located in Leninogorsk region, Romashkinskoye (UVRT) and natural control reserve site in Raifa, Tatarstan Republic, Russia on pine forests by applying stable carbon isotope analysis in pine tree-rings ($\delta^{13}C_{ptrw}$). Our results show decreasing $\delta^{13}C_{ptrw}$ at UVRT in 1943, when oil extraction was started and in 1970, when it is reached the maximum production. We found that $\delta^{13}C_{ptrw}$ from UVRT indicates on developing unfavourable drier conditions and suppressed tree growth caused by both human-induced oil and deposit infrastructure and natural processes compared to undisturbed Raifa site. A 5-year running correlation analysis showed significant difference between sites in 1965 over the period 1930 to 2021. The $\delta^{13}C_{ptrw}$ values from Raifa are more negative compared to UVRT, which can be explained by higher forest sensitivity to human-induced impact. From eco-physiological point of view decreasing of intercellular (c_i) to ambient (c_a) CO_2 concentrations ratio at the leaf level and increasing intrinsic water use efficiency (iWUE) along with decreasing tree-ring width at UVRT (1970-2021) indicate on developing of drought conditions.

Keywords: CO_2; CH_4; $\delta^{13}C$ in tree-ring wood; soil; iWUE; climate

1. Introduction

Accelerated development of energy resources around the world has significantly increased forest change associated with oil and gas activities, leading to both carbon dioxide and methane emissions. The impacts of these anthropogenic indirect greenhouse gases (GHG) play a significant role on forest ecosystems at the regional and global scales [1]. The GHG attributed up to 65 % to human activities [2], including hydrocarbon emissions from the oil and gas infrastructures [3] causing a global average air temperature increases by 1.4°C [4]. Moreover, the extraction and refining of oil produces about 48% of hydrocarbons and 44% of carbon monoxide [5], which can significantly impact the environment. In case of accidents or during intensive oil and gas deposit development the toxic contamination of soil can lead to reduction of air exchange in the soil hindering the water flow into the soil compared to the clean natural soils. Water shortage in the soil can lead to soil fertility and reduction of microbial activity impacting forest ecosystem negatively. Additionally, local oil and gas production delivers up to 90% of hydrocarbons, which contribute to the global GHG emissions [6]. Due to intensive development of oil and gas depositions, oil and oil products refining the problem of their emissions locally and globally impacting the environment and humans' health.

Recent climate change and drought-induced trees mortality affect forest ecosystems worldwide [7]. It is well known that forest soils and permafrost are important sink for atmospheric methane

emissions, where a GHG is contributing roughly 20% to the global warming [8,9]. Soil microorganisms remove about 30 million tons of GHG from the atmosphere annually, which is 6 - 10% of its annual flow [10]. Living and dead trees have the potential to be CH_4 sources or sinks or both [9]. Different tree species have different effects on the activity of CH_4 oxidation in the soil - the highest is noted under *Pinus cembra* L. (27.68 mg kg^{-1}) in Europe, in *Larix sibirica* Led. (7.98 mg kg^{-1}), *Pinus sylvestris* L. (4.96 mg kg^{-1}) and the lowest - in spruce (4.62 mg kg^{-1}) forest [10].

The carbon atoms fixed in tree-ring width originated from the atmospheric carbon dioxide to which the tree's canopy is exposed [9]. During photosynthesis several fractionation steps take place, first when CO_2 from the atmosphere (c_a) diffuses into the leaf (needle) intercellular spaces (c_i), and second during CO_2 fixation by the enzyme Rubisco [11]. The opening and closure of stomata (g_s) determines the water control. Under warm and dry conditions trees respond to limited water resources by reducing stomatal conductance (g_s), resulting in decreasing CO_2 uptake and biomass production, in reduced intercellular CO_2 concentration (c_i). Changes in the assimilation rate of the needles will therefore influence the intercellular CO_2 concentration (c_i) through changes of the rate at which the CO_2 is utilized to form sugars and an increase or decrease in stomatal conductance will affect the rate at which this internal CO_2 (c_i) can be replenished. Trees discriminate more strongly against ^{13}C under conditions of high (c_i), when stomata are relatively wide open, or photosynthesis is low [11]. Under increasing CO_2 concentration, the water vapor exchange between the needles and the ambient air (c_a) is reduced and stomatal conductance decreases [12–14]. The carbon isotopic ratio ($^{13}C/^{12}C$ or $\delta^{13}C$) in tree rings reflects signals of water availability and air humidity as a result of the impact of climate on photosynthesis. Atmospheric CO_2 is well mixed, but the sub-canopy air space can become depleted in ^{13}C due to inputs from soil and plant interaction. Tree growth is influenced by many factors such as solar irradiance, ambient air temperature, precipitation, air humidity, soil and ground water, nutrient availability as well as water. The heavier stable carbon isotope (^{13}C) in tree rings is modulated by environmental parameters like temperature and moisture regime changes due to fractionation processes during CO_2 uptake as well as those related to land management, disturbances like insects [7,11,12,14–16]. Photosynthetic limitations of intrinsic Water Use Efficiency (iWUE) can be an indicator for oil refinery in case of increase, which correspond with NOx pollution [17] and moisture changes, reducing climate sensitivity [18]. If trees uptake a significant amount of hydrocarbon emitted from the gas and oil deposits, then we suggest that tree-ring $\delta^{13}C$ should also get more negative values.

Data on hydrocarbon (HC) production are available for the study area, however, it is not possible to estimate how much hydrocarbons are released from gas and oil deposits into the air, surface water, groundwater, and soil. The HC emissions most likely occur from the subsurface prior the oil and gas deposit development. It was relatively constant flow, for hundreds of thousands and even millions of years, which could change only in case of any events like earthquakes [19]. But after the beginning of the field development, the equilibrium established during a long geological time was broken that could lead to an increase in the flow of hydrocarbons both from natural fractures and faults and due to losses during production and transportation. In the first stage of extraction, oil is extracted through natural processes. As a result, it is replaced by water. If the pressure in the reservoir does not allow oil to come to the surface, then special pumps are used to extract it. Later, secondary methods are used to extract oil. It is carried out by introducing liquids and gases into oil-bearing formations to provide the necessary amount of energy to extract oil from the earth's bowels [20]. At this stage of production, the natural state of the reservoirs is disturbed and a significant emission of hydrocarbons into the air, water and soil is possible. When using the hydraulic fracturing method, HC emissions can be very large, comparable to other global sources of greenhouse gases [21]. A large increase in U.S. methane emissions over the past decade inferred from the satellite data and surface observations [22,23].

In the Romashkinskoye UVRT field, the hydraulic fracturing method was not used, but there could also have been noticeable HC emission during the production. Methods for assessing hidden HC emission during oil field development were not developed. Usually, only accidents in which a large volume of HC is released into soil or water are evaluated.

 doi:10.20944/preprints202310.0090.v1

In this study, we hypothesized that during oil and gas deposit developments and active oil production additional emission of hydrocarbons can be emitted into the atmosphere, which can be recorded in trees growing close to the oil and gas deposit site.

To test this hypothesis, we developed new tree-ring $\delta^{13}C$ in pine wood chronologies from the oil and gas deposits (UVRT) and for the control natural reserve Raifa (Raifa) site to reveal impact of Romashkinskoye oil and gas deposit site on the pine forests.

2. Materials and Methods

2.1. Study sites

Study sites are located in the Republic of Tatarstan within 54-55° N and 49-52° E, Russian Federation. We investigated two sites: UVRT - the oil and gas deposit infrastructure (UVRT) site near to Romashkinskoye deposit industrial site and Raifa – a control natural reserve site, which is located 250 km away from the UVRT (Figure 1a). The territory is located on the southern border of taiga natural zone in the Volga-Vyatka high-plain complex of dark coniferous-broad-leaved forests [22].

The Romashkinskoye UVRT oil and gas deposit site is located 54° N, 52° E, which is 15 km away from Almetyevsk city in the northwestern part of the Bugulma plateau, confined to the South Tatar (Almetyevsk) arch at 200-210 m asl (Figure 1a). Geological oil reserves are 5 billion tons, while proved and recoverable reserves - 3 billion tons. Exploratory drilling was started in 1943 [19,20], while in 1948 a thick Devonian formation was discovered. Intensive development and exploitation were started in 1953. At present the Romashkinskoye field is one of the largest oil fields in the world. More than 400 deposits have been identified; the main ones in terms of size: oil deposits of the Devonian terrigenous complex in the Kynovsko-Pashy sediments, this is about 70% of the explored reserves. Reserves replenishment: commercial oil reserves are growing, although cumulative production is also growing and already exceeds previously approved reserves. Depletion of sediments of the Pashinsky horizon of the Romashkinskoye field is regularly estimated at more than 85%. It is announced that residual oil reserves are concentrated in undeveloped low-permeability reservoirs. Then petrophysical works, hydrodynamic studies, seismic exploration are carried out, and the reserves are replenished. The composition of the Kynovsko-Pashy sediments indicates that anomalous zones of light oil from the Zhivet complex flowed into the wells. The Zhivetsky complex is represented by sandstones, siltstones and clays with thin interlayers of marls and limestones and is divided into Afoninsky and Starooskolsky horizons [19,21].

The relief of the study site is characterised as a flat with small hills. Dry forest dominated by pine (*Pinus sylvestris* L.) (Figure 1b). The herbage is dominated by ground reedgrass, sedges and various steppe plant species. The soils are dry sod-podzol soils on sandy and sandy loam sediments.

The Raifa natural reserve (control) site 55° N, 49° E (Figure 1a) is represented by pine trees as the main dominant species (*Pinus sylvestris* L.) (Figure 2c), while rarely spruce and birch (green-moss pine forest). Pine trees (*Pinus sylvestris* L.) can reach up to 150 years. The forest stand encounters single species of *Betula pendula* Roth., *Picea fennica* (Regel) Kom. The understory is sparse, represented by *Euonymus verrucosus* Scop., *Tillia cordata* Mill. Dominants of the herbaceous layer are *Calamagrostis epigejos* (L.) Roth and *Convallaria majalis* L. The soil is soddy-podzolic on sandy and sandy loam deposits of the third floodplain terrace of the Volga River [22].

2.2. Local weather station observations

The climate of the region is continental with cold winters and warm summers. According to the local Kazan weather station (55° N, 49° E) average annual temperature is 5.2°C, January average temperature reaches -10.4°C, July average temperature is 20.8°C for the period from 1970 to 2021. Average snow depth in winter reaches up to 40 cm. Sum of precipitation is 584 mm per year. Maximum precipitation falls in July up to 70 mm, minimum is recorded in March up to 33 mm according to the average monthly data from Russian Research Institute of Hydrometeorological Information – World Data Center [23] for the period from 1970 to 2021.

 doi:10.20944/preprints202310.0090.v1

2.3. Sampling

Tree core sampling from four dominant pine trees (*Pinus sylvestris* L.) was carried out in July 2022 at each study location (UVRT and Raifa). Pine tree cores were collected at a height of 1.3 m at the breast hight on the south- and north- side of the tree from visually healthy, without double crown and not damaged living *Pinus sylvestris* L. trees using Pressler increment borer (Figure 1b,c) according to the standard methodology [24]. All tree cores were packaged in the metal foil and placed in a hard tube for transportation to the stable isotope laboratory.

Soil samples were collected in February-March 2023 using a soil drill borer. The depth of sampling ranged from 1.0 to 1.5 m [24]. Soil samples were placed in a glass container immediately after extraction from the pits, filled with salt solution and hermetically sealed.

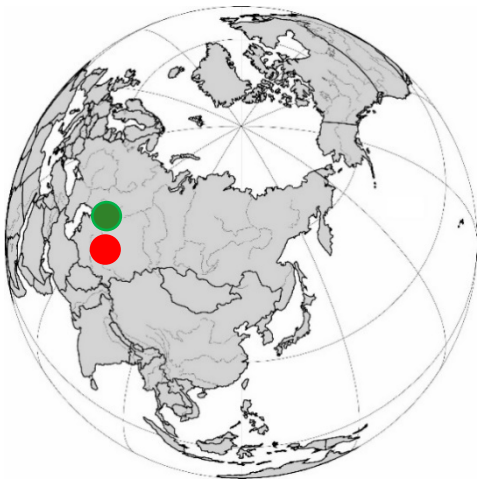

(**a**)

Preprints (www.preprints.org) | NOT PEER-REVIEWED | Posted: 3 October 2023 doi:10.20944/preprints202310.0090.v1

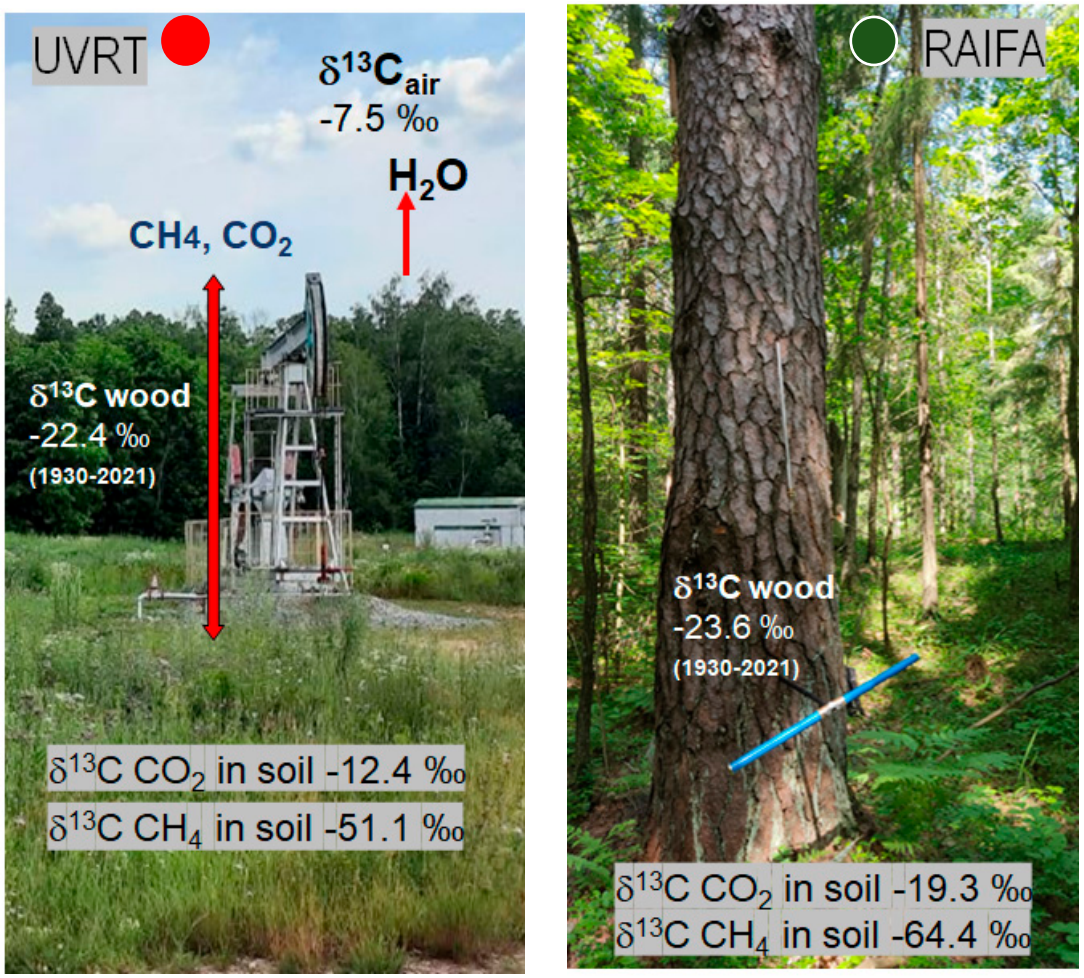

(**b**) (**c**)

Figure 1. Schematic map location (**a**) and photos from (**b**) oil and gas deposits infrastructure UVRT (red circle) and (**c**) natural reserve Raifa (green circle) sites. Averaged numbers of the $\delta^{13}C$ atmospheric CO_2 [25] and $\delta^{13}C_{ptrw}$ are presented for the period from 1930 to 2021. The $\delta^{13}C$ CO_2 and $\delta^{13}C$ CH_4 are presented for the year of 2023 with schematic interaction of water evaporation and CH_4 and CO_2 soil-atmosphere-plant exchange.

2.4. Tree-ring width and stable isotope analyses

Tree-ring widths (TRW) were measured for the UVRT site for the period from 1925 to 2022 and for Raifa for the period 1887 to 2021 using a Lintab-6 with the TSAPWin software package [26]. The quality of the cross-dating chronologies was assessed by using the Cofecha software [27,28]. After that each annual tree-ring was split using a sharp BA-170P NT blade under a Leica M50 microscope.

For the stable carbon isotope analysis, each annual tree-ring sample for each year separately was packed ca. 200 μg into capsule. All measurements for each sample were repeated three times. IAEA standards were used as a reference sample for control: USGS-40 and IAEA-CH-7 with known carbon isotopic ratios.

Stable carbon isotope measurements in wood samples were performed for each tree and each year separately using a Delta V Plus isotope mass spectrometer (Thermo Fisher Scientific, Germany) via a Flash HT Plus in constant flow mode at the Kazan Federal University. Tree-ring $\delta^{13}C$ in wood chronologies were corrected according to $\delta^{13}C$ atmospheric CO_2 for both study sites.

The $\delta^{13}C$ CO_2 and $\delta^{13}C$ CH_4 in soil samples were analysed for both sites using Delta V Plus (Thermo Fisher Scientific, Germany, SN08893D). Gas samples were separated and prepared using a TRACE 1310 gas chromatography-mass spectrometer (ThermoFisher Scientific, Germany, 713101387) coupled with an ISQ quadrupole mass detector (ThermoFisher Scientific, USA) connected to the

Preprints (www.preprints.org) | NOT PEER-REVIEWED | Posted: 3 October 2023 doi:10.20944/preprints202310.0090.v1

isotope mass spectrometer via a GC Isolink interface unit. Gas sample was injected automatically by means of the TriPlus RSH autosampler (CTC Analytica AG, Switzerland) from the vial with gas with a gas-tight syringe and introduced into the chromatograph evaporator, the syringe was purged with pure helium before sampling. The volume of the injected sample varied from 0.1 mL to 2.5 mL depending on the content of the target gases in the sample. Two chromatographic columns were used for complete separation of methane, carbon dioxide, and air group gases (which interfere with the determination of the carbon isotopic ratio due to interference with nitrogen oxides). The results were processed using the "Isodat" data processing program [29].

The stable carbon isotopic ratio ($^{13}C/^{12}C$) is typically expressed in delta notation as ($\delta^{13}C$) (Equation 1), which is the relative deviation of the ratio in the organic sample (R_{sample}) from that of an internationally accepted standard ($R_{standard}$), Vienna Pee Dee Belemnite (VPDB).

$$\delta_{sample} = (R_{sample} - R_{standard} - 1)*1000 \quad (1)$$

2.5. CO_2 and greenhouse gas emissions (GHG)

Correction of raw tree-ring $\delta^{13}C$ is necessary because the combustion of fossil fuels and biomass and land-use changes have resulted in a decrease in $\delta^{13}C$ of the atmospheric CO_2 over the last 150 years. Changes in the isotopic ratio of atmospheric CO_2 are directly reflected in the isotopic ratios of the products of photosynthesis. Calculating the differences for each year to the pre-industrial value (1850) for $\delta^{13}C$ of atmospheric CO_2 obtained from ice cores and direct atmospheric measurements at the Mauna Loa Observatory, Hawaii [25; https://gml.noaa.gov/ccgg/trends/] we subtracted these differences from the raw isotope series for $\delta^{13}C$ values for each year. Because isotope fractionation is additive, this completely removes the trend due to decreasing atmospheric $\delta^{13}C$ from fossil fuel emissions and land-use changes.

Local data from the oil extraction and cumulative oil production from the gas and deposite UVRT site are available for the period 1943 to 2021 [19] for comparison with our newly developed $\delta^{13}C$ptrw from UVRT and controlled natural reserve Raifa site. Global oil and gas emissions data from Russia and globally [6] were used for regression analysis with $\delta^{13}C_{ptrw}$ from both UVRT and Raifa sites.

2.6. Relation to intrinsic water-use efficiency (iWUE)

The calculation of intrinsic water-use efficiency (iWUE) was based on the Equation (2) described in detail by Saurer and Voelker [30,31].

$$iWUE = ca*(b - (\delta^{13}Catm - \delta^{13}Cplant)/1.6*(b - a) \quad (2)$$

where ca— is the ambient CO_2 concentration, c_i – is the intercellular CO_2 concentration, and 1.6 is the ratio of water diffusivities and CO_2 in the air. Diffusion through the stomata is described as (a = 4.4‰), b is the discrimination associated with carboxylation (b = 27‰) [13,31].

The $\delta^{13}C_{plant}$ is uncorrected tree-ring $\delta^{13}C$ measurements in pine wood relative to the $\delta^{13}C$atm atmospheric CO_2. The $\delta^{13}C_{atm}$—data is available from https://www.esrl.noaa.gov/gmd/outreach/isotopes/c13tellsus.html (accessed on 22 March 2023).

2.7. Statistical analyses

The statistical analysis was performed in the STATISTICA Ultimate Academic 13 RUS / EN Rus for Window). The mean, minimum, maximum values, standard deviation (SD), Pearson correlation coefficients were calculated for stable carbon isotope chronologies from both study sites. A 5-year running correlation analysis was performed between $\delta^{13}C_{ptrw}$ from UVRT and Raifa site to reveal a breakpoint and differences between control and oil and deposit sites. Stable carbon isotope chronologies for both study sites were detrended using time series forecasting analysis with the "no trend" function. Multiple regression analysis was were performed between local and global gas and oil emissions versus $\delta^{13}C_{ptrw}$. D**ependent variable was associated with $\delta^{13}C_{ptrw}$, while independent variables were local and global oil gas emissions. Bivariant regression plots were computed.**

Preprints (www.preprints.org) | NOT PEER-REVIEWED | Posted: 3 October 2023 doi:10.20944/preprints202310.0090.v1

Pearson correlation matrix was computed and correlation analysis between non-detrended, detrended tree-ring $\delta^{13}C_{ptrw}$ from both study sites UVRT and Raifa with the climatic parameters from the local Kazan weather station was performed. Monthly averaged temperature (T) and precipitation (P) data from September of the previous year (T, P_9) to August of the current year (T, P_8), annual air temperature and precipitation data (T1_12; P_1_12), averaged spring-summer (T,P_4567), summer (T,P 678) were used for calculations.

To reduce impact of trends we use detrended stable isotope chronologies. The level of statistical significance is expressed as a *P-value* ≤ 0.05.

The iWUE data were smoothed by a 11-year Hamming window [32] to reveal low-frequency variations and to compare long-term trends between study sites.

2.8. Spatial climate patterns

Spatial correlation gridded maps were computed within the gridded net 0.5 x 0.5° within the coordinates 50-60°N, 40-55°E between June-August evapotranspiration, differences between maximal und minimal air temperature ($T_{max-min}$), precipitation, and cloud fraction available at the KNMI Climate Explorer https://climexp.knmi.nl/ (accessed date on 29 March 2023) and detrended tree-ring $\delta^{13}C_{ptrw}$ from UVRT site for the period 1980-2020. The level of significance *P-value ≤ 0.05*.

3. Results

3.1. Stable carbon isotopes in wood vs. oil and gas emissions

Stable carbon isotope chronologies were developed for UVRT and Raifa sites based on four individual trees for each study site for the common period from 1930 to 2021 (Figure 2a).

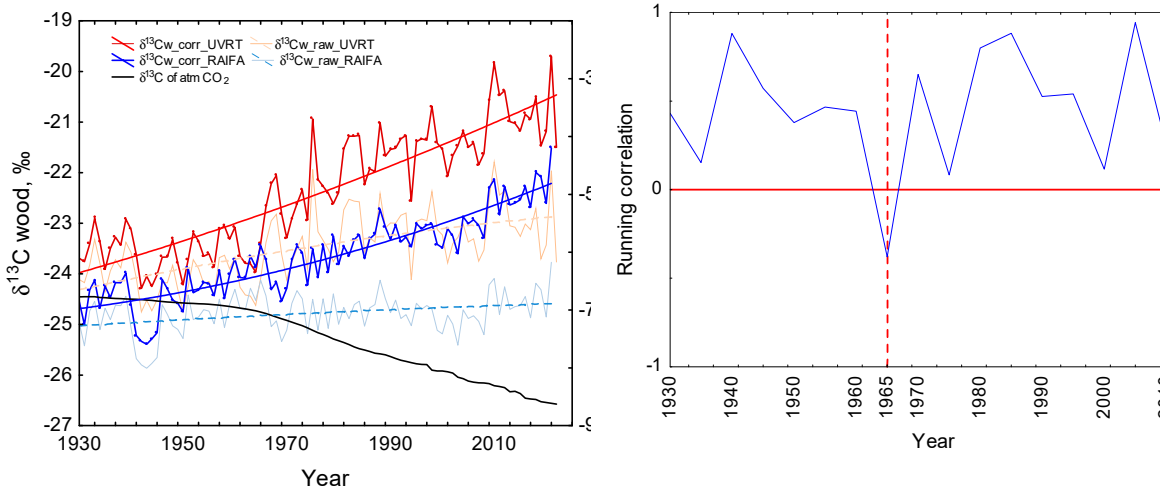

(**a**) (**b**)

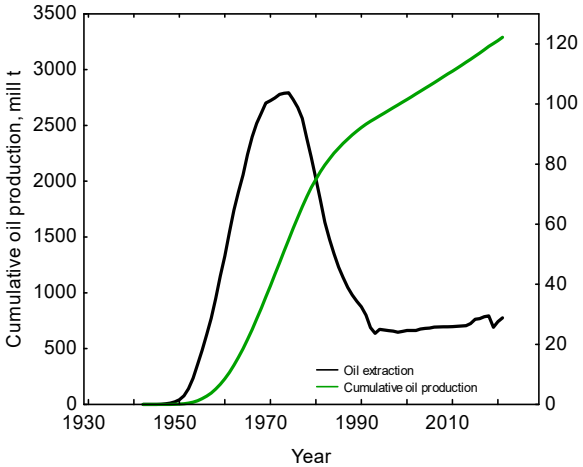

Preprints (www.preprints.org) | NOT PEER-REVIEWED | Posted: 3 October 2023 doi:10.20944/preprints202310.0090.v1

(**c**)

Figure 2. Raw (light blue and light red lines) and corrected (bold blue and bold red lines) according to $\delta^{13}C$ of atmospheric CO_2 [29] tree-ring $\delta^{13}C$ in pine wood chronologies ($\delta^{13}C_{ptrw}$) from UVRT (red colour lines) and Raifa (blue colour lines) sites versus $\delta^{13}C$ atmospheric CO_2 (bold black) from 1930 to 2021 (**a**). A 5-year window running correlation between $\delta^{13}C_{ptrw}$ from UVRT and Raifa sites. The break point year is represented as the dotted line in 1965 (**b**). Oil extraction (black line) and cumulative oil production (green line) from Romashkinskoye oil and gas deposit [19] for the period from 1943 to 2022 in comparison with δ^{13}Cptrw from UVRT and Raifa (**c**).

The mean $\delta^{13}C$ value is more negative for Raifa (-23.6‰) compared to UVRT (-22.3‰). Standard deviation (SD) is higher for the UVRT site (1.2) compared to Raifa (0.8). Maximum and minimum values are more negative for Raifa (max -21.5‰, min -25.4%) compared to UVRT (max -19.7‰, min -24.3‰). The $\delta^{13}C$ from Raifa showed significant correlation with UVRT ($r = 0.89$, $P < 0.001$). Moreover, we found more negative values for both $\delta^{13}C$ CO_2 and $\delta^{13}C$ CH_4 in soil samples from Raifa site (-19.3 ‰ and -64.4 ‰) compared to UVRT (-12.4 and -51.1 ‰), respectively.

A 5-year running correlation analysis between δ^{13}Cptrw from UVRT and Raifa (Figure 2b) showed significant difference in the year of 1965, showing negative correlation ($r = -0.38$; $P < 0.05$) over the studied period 1930-2020. During other subperiods positive correlations were revealed.

The oil and gas extraction from the deposits started in 1943 and reached maximum in 1970 (Figure 2c), which correspond with decreasing $\delta^{13}C$ values from both study sites with the most pronounced decrease for Raifa natural reserve site (Figure 2a).

Regression analysis showed significant relationships between local Romashkinskoye oil extraction and detrended stable carbon isotope chronologies for UVRT and Raifa sites ($r^2 = 0.19$ and $r^2 = 0.04$), respectively (Figure 3ab), with higher significant correlation for the gas and oil deposit UVRT site only.

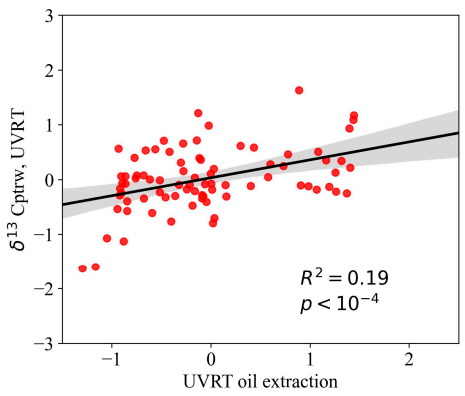

(**a**)

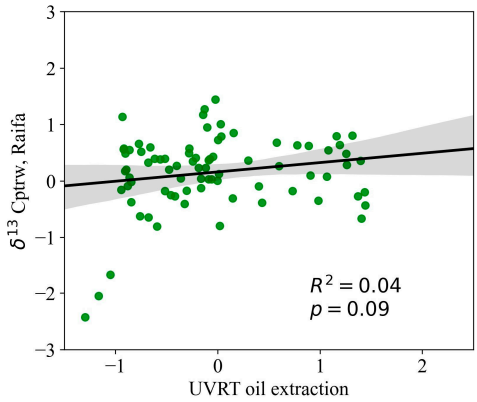

(**b**)

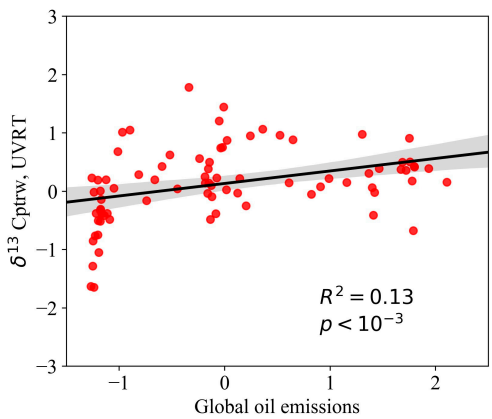

(**c**)

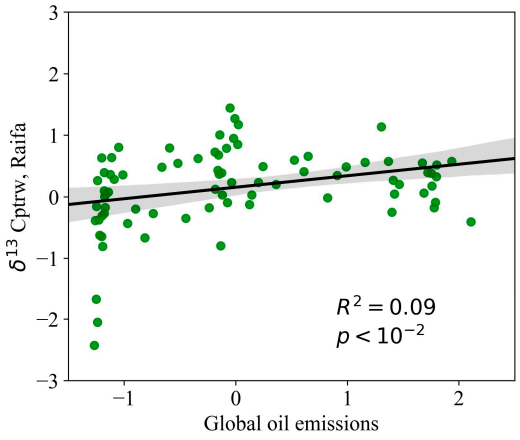

(**d**)

Preprints (www.preprints.org) | NOT PEER-REVIEWED | Posted: 3 October 2023 doi:10.20944/preprints202310.0090.v1

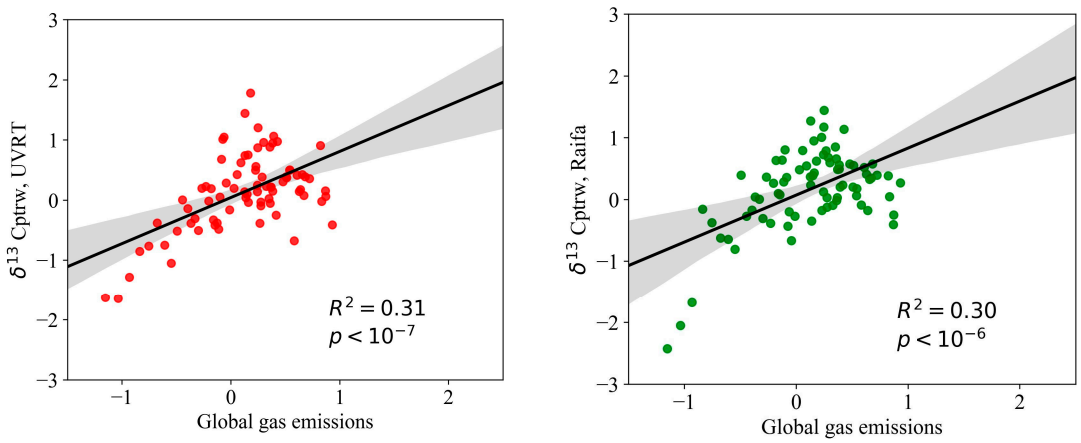

(**e**) (**f**)

Figure 3. Detrended tree-ring $\delta^{13}C_{ptrw}$ from the UVRT (left panel) and Raifa (right panel) sites versus detrended local Romashkinskoe oil extraction [19] (**a-b**), global oil (**c-d**) and gas (**e-f**) [6] emissions for the period 1943 to 2021. Confidential interval is 0.95, $P < 0.05$.

The global oil and gas emissions correlate significantly with tree-ring $\delta^{13}C_{ptrw}$ for UVRT ($r^2 = 0.13$; $r^2 = 0.31$) (Figure 3c,e) and for Raifa ($r^2 = 0.09$; $r^2 = 0.30$) (Figure 3d,f), $P < 0.05$, respectively.

3.2. Intrinsic water use efficiency (iWUE) versus tree-ring width and tree-ring $\delta^{13}C$

Earlier 1930s averaged tree-ring width (TRW) chronology from UVRT shows lower mean values (1.42 mm) and SD (1.21) compared to Raifa site for TRW (1.55 mm) and SD (1.44), respectively. However, starting from 1960s tree-ring width from Raifa showed higher values, compared to supressed UVRT site (Figure 4a).

Intercellular CO_2 concentration (c_i) showed higher offset between two sites starting from 1965, when oil and gas production from Romashkinskoye is double increased (Figure 4b) with higher c_i for Raifa site. Lower c_i values were found for the UVRT site can be explained by stomata closure and incorporating higher CO_2 concentration leading to drier conditions.

Strong decreasing c_i/c_a trend with lower values (Figure 4c) and continuous increase of iWUE (Figure 4d) were revealed for UVRT site. Both UVRT and Raifa showed similar increasing trends from 1930 towards 2020 (Figure 4d).

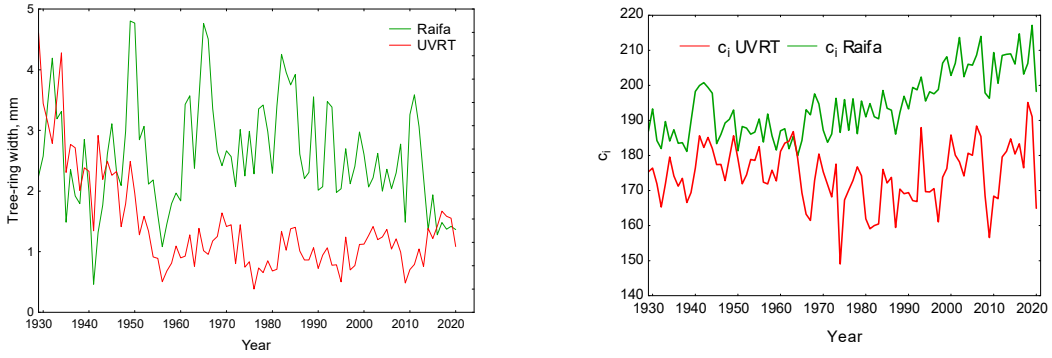

(**a**) (**b**)

Preprints (www.preprints.org) | NOT PEER-REVIEWED | Posted: 3 October 2023 doi:10.20944/preprints202310.0090.v1

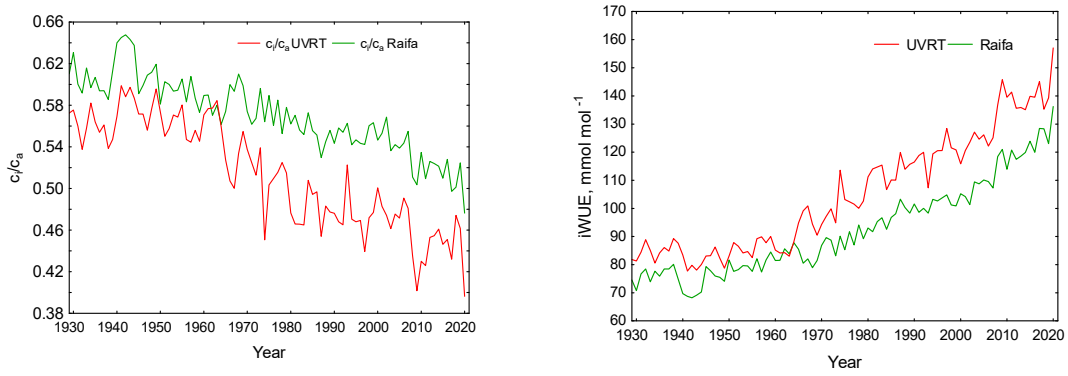

(**c**) (**d**)

Figure 4. Averaged tree-ring width chronologies (**a**), intercellular CO_2 concentration (c_i) (**b**) and intercellular CO_2 concentration versus ambient CO_2 concentration (c_i/c_a) from Raifa versus oil and gas reservoirs UVRT site (**c**). Intrinsic Water Use Efficiency (iWUE) calculated for both Raifa and UVRT study sites (**d**).

3.3. Impact of local environmental parameters on tree-ring $\delta^{13}C$ variability

Pearson correlation analysis betweennon-detrended and detrended tree-ring $\delta^{13}C_{ptrw}$ from both study sites showed positive significant ($P < 0.05$) correlations with spring-summer air temperature (April - July) (r = 0.65; 0.52) for Raifa and (r = 0.61; 0.45) for UVRT site respectively.

The highest correlation was found between annual air temperature between non-detrended $\delta^{13}C_{ptrw}$ for Raifa (r = 0.74) and for UVRT (r = 0.68) (Figure 5). Detrended $\delta^{13}C_{ptrw}$ showed lower values, but still significant correlations (r = 0.44) for Raifa and for UVRT (r = 0.31).

A negative significant correlation was found between tree-ring $\delta^{13}C$ from Raifa and summer (June-August) precipitation (r = - 0.21; $P < 0.05$). Positive significant correlations were found between detrended $\delta^{13}C_{ptrw}$ from both sites with spring air temperature and precipitation of the previous year and the current one.

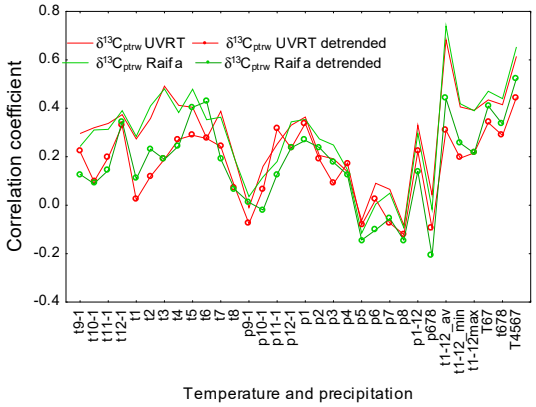

Figure 5. Pearson correlation analysis between $\delta^{13}C_{ptrw}$ chronology from UVRT (red line), $\delta^{13}C_{ptrw}$ chronology from Raifa (green line) as well as detrended $\delta^{13}C_{ptrw}$ from UVRT (red line with circle) and $\delta^{13}C_{ptrw}$ from Raifa (green line with green circle) versus climatic data from the local Kazan weather station. Temperature and precipitation from September of the previous year are marked as T9-1 and P9-1, respectively. Monthly averaged temperature and precipitation are indicated in numbers.

3.4. Spatial correlations patterns

Detrended tree-ring $\delta^{13}C$ chronology from UVRT site showed positive significant ($P< 0.05$) spatial correlations within gridded net 0.5x0.5° for the coordinates within 50-60°N, and 40-55°E with averaged June-August evapotranspiration (r = 0.5) (Figure 6a) and June-August $T_{max-min}$ (r = 0.5)

Preprints (www.preprints.org) | NOT PEER-REVIEWED | Posted: 3 October 2023 doi:10.20944/preprints202310.0090.v1

(Figure 5b), while negative with June-August precipitation (r = -0.5) (Figure 6c) and June-August cloud fraction (r = -0.6) (Figure 6d).

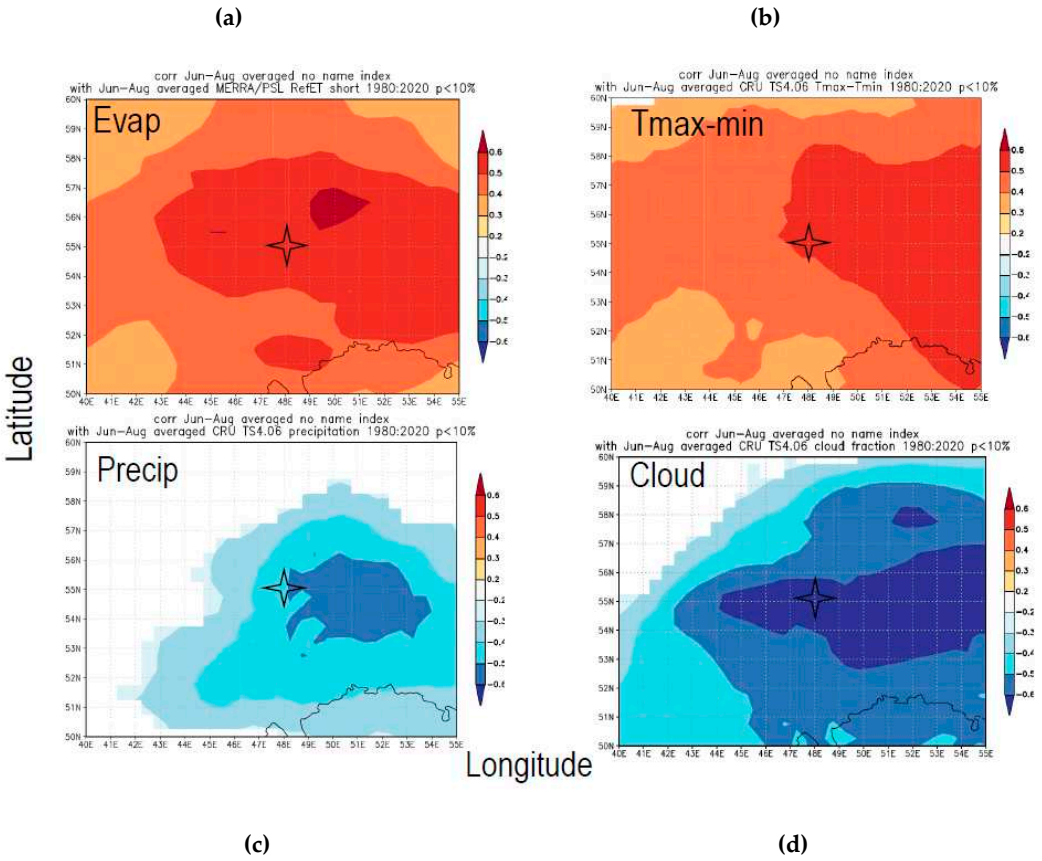

Figure 6. Spatial distribution of correlation coefficients within gridded 0.5x0.5° net coordinates 50-60°N, and 40-55°E between detrended tree-ring $\delta^{13}C_{ptrw}$ from UVRT and averaged June- August reference evapotranspiration (**a**), differences between maximal and minimal air temperature ($T_{max-min}$) (**b**), precipitation (**c**) and cloud fraction (**d**) computed for the period from 1980-2020. Right vertical scales represent correlation coefficients within the range from − 0.6 (dark blue, negative correlations) to +0.6 (dark red, positive correlations) with the $P < 0.05$.

4. Discussion

The oil and gas industry started to be developed in Romashkinskoye, the Tatarstan Republic, Russian Federation since 1943 [19] and in 1970s reaches the maximum in oil extraction, which was recorded in tree-ring pine $\delta^{13}C_{ptrw}$ chronologies from both UVRT and Raifa sites. Recently the oil and gas production were increased by 3.5 % compared to the past. Further increase of oil and gas production is expected in the near future [33]. Accelerating rate of GHG emissions will undouble will change the environment, biodiversity and humans' health. Only accidents in which a large volume of hydrocarbons released into the soil or water have been evaluated so far. Therefore, our pioneering study is highlighting how trees could respond to oil and gas development infrastructure near to the deposit and in remote sites location of the region.

Our results at the tree-ring level show higher tree growth suppression during the oil extraction for the UVRT site, which is also reflected in the tree-ring $\delta^{13}C$ values. This can be explained by the negative impact of developed oil and gas infrastructure on the pine forest. Our finding is in line with Pickell et al. [34], who showed anthropogenic disturbance in developed oil and gas activities on forest landscapes in the USA [35]. The heavier stable carbon isotope (^{13}C) in tree rings is modulated by hydrocarbon emissions from the infrastructure site, additionally to environmental parameters like temperature, precipitation, sunshine duration, and evapotranspiration. Moreover, anthropogenic

 doi:10.20944/preprints202310.0090.v1

CO_2 increase due to Suess effect and global GHG emissions accumulated in tree rings, which is reflected in drastic $\delta^{13}C$ increase towards the recent decades.

Interestingly, pine trees from the natural reserve Raifa site, which is undisturbed by direct human impact show more positive tree-ring with variability compared to the human-induced UVRT site. However, tree-ring $\delta^{13}C$, CH_4 and CO_2 in soil showed more negative values compared to the oil and gas deposits UVRT site. One of the explanations can be that pine trees from natural reserve site are more sensitive to the impact of greenhouse emissions, while pine trees from the human-induced site are already stressed by the local and global impact. Significant impact of local oil extraction and global HC emissions was revealed for UVRT site, which supports our hypothesis that both local and global hydrocarbon emissions affect local pine forests. Increasing of intrinsic water use efficiency (iWUE) along with decreasing tree-ring width chronology from the oil and gas deposits indicate on developing of drought conditions (Figure 4) during the vegetation period, which is confirmed by the local and spatial climatic correlation analyses. Despite site-specific and species-specific differences study by Guerrieri et al. [17] showed that NOx pollutions alter the iWUE by confirming impact of anthropogenic factors on oak trees. It is well known that variation of c_i depends on various environmental factors and on species and site conditions. Our study demonstrates site-specific response of trees to oil and gas production after 1965 showing an offset between two sites. The c_i/c_a ratio decreases toward recent decades, indicating the closure the stomata, which is also reflected in increased iWUE trends for both sites. However, higher iWUE is observed for the control natural reserve Raifa site.

Increasing evapotranspiration and extreme changes in air temperatures, less clouds and decreasing of precipitation lead to developing drier environmental conditions. Pine trees from Raifa site record more pronounced drought conditions during July over the period from 1970 to 2021, which is also recoded in $\delta^{13}C_{ptrw}$ values. Early spring temperatures can impact tree growth significantly, by shifting vegetation period to earlier dates. Such of early spring temperature shift was observed for southern part of Siberia due to early snowmelt under recent anthropogenic warming [36,37]. However, here is challenging to separate impact from the global and local anthropogenic emissions. Therefore, further studies are needed for complex and multi-parameter approaches.

5. Conclusions

We conclude that pine trees from UVRT site indicate on developing unfavourable drier conditions and suppressed tree growth caused by both human-induced oil and deposit infrastructure and natural eco-physiological processes compared to the undisturbed natural reserve Raifa site.

Based on our pilot study we would recommend performing seasonal and annual multi-proxy parameters approaches by analysing $\delta^{13}C$ in needles, $\delta^{13}C$ and CH_4 in the soil at the different depths; and analysing tree-ring cellulose instead of wood, which is more sensitive parameter to both eco-physiological and climatological changes. Further local oil and gas developments and their impacts on forest ecosystems should be better tracked and analysed along the transect for long-term monitoring.

Understanding the mechanisms behind of local hydrocarbon emissions from the oil and gas deposits and their contribution to the global GHG emissions is of great importance and should be further investigated among transects and comparing with other available oil and gas deposits infrastructures in the region locally and globally.

Author Contributions: Conceptualization all authors; methodology G.B.; B.G.; G.M; A.T.; D.T; D.K.; D.N.; software O.V.Ch.(S).; G.M.; validation, O.V. Ch. (S); G-M.; formal analysis O.V. Ch. (S); G-M.; A.T.; D.T; G.B.; B.G.; resources D.N.; data curation O.V. Ch. (S); writing—original draft preparation all authors; writing—all authors; visualization O.V. Ch. (S); supervision D.N.; project administration, D.K..; funding acquisition, D.N. All authors have read and agreed to the published version of the manuscript.

Funding: This research was funded by the Kazan Federal University Strategic Academic Leadership Program (PRIORITY-2030).

Data Availability Statement: Research data will be uploaded in Zenodo repository upon acceptance of the manuscript.

Acknowledgments: This research was funded by the Kazan Federal University Strategic Academic Leadership Program (PRIORITY-2030).

Conflicts of Interest: The authors declare no conflict of interest.

References

1. Jones, M. W.; Peters, G.P.; Gasser, T.; Andrew, R.M.; Schwingshackl, C.; Gütschow, J.; Houghton, R.A.; Friedlingstein, P.; Pongratz, J.; Le Quéré, C. National contributions to climate change due to historical emissions of carbon dioxide, methane, and nitrous oxide since 1850. *Scientific Data*, **2023**, 10(1), pp. 1-23, https://doi.org/10.1038/s41597-023-02041-1.
2. Saunois, M.; Bousquet, P.; Poulter, B.; Peregon, A.; Ciais, P.; Canadell, J.G.; Dlugokencky, E.J.; Etiope, G.; Bastviken, D.; Houweling, S.; Janssens-Maenhout, G.; Tubiello, F. N.; Castaldi, S.; Jackson, R. B.; Alexe, M.; Arora, V. K.; Beerling, D. J.; Bergamaschi, P.; Blake, D.R.; Brailsford, G.; Brovkin, V.; Bruhwiler, L.; Crevoisier, C.; Crill, P.; Covey, K.; Curry, C.; Frankenberg, C.; Gedney, N.; Höglund-Isaksson, L.; Ishizawa, M.; Ito, A.; Joos, F.; Kim, H.-S.; Kleinen, T.; Krummel, P.; Lamarque, J.-F.; Langenfelds, R.; Locatelli, R.; Machida, T.; Maksyutov, S.; McDonald, K. C.; Marshall, J.; Melton, J. R.; Morino, I.; Naik, V.; O'Doherty, S.; Parmentier, F.-J.W.; Patra, P.K.; Peng, C.; Peng, S.; Peters, G.P.; Pison, I.; Prigent, C.; Prinn, R.; Ramonet, M.; Riley, W.J.; Saito, M.; Santini, M.; Schroeder, R.; Simpson, I.J.; Spahni, R.; Steele, P.; Takizawa, A.; Thornton, B.F.; Tian, H.; Tohjima, Y.; Viovy, N.; Voulgarakis, A.; van Weele, M.; van der Werf, G.R.; Weiss, R.; Wiedinmyer, C.; Wilton, D.J.; Wiltshire, A.; Worthy, D.; Wunch, D.; Xu, X.; Yoshida, Y.; Zhang, B.; Zhang, Z.; Zhu, Q. The global methane budget 2000–2012. *Earth Syst. Sci Data*, **2016**, 8, pp. 697–751, https://doi.org/10.5194/essd-8-697-2016.
3. Bruhwiler, L. M.; Basu, S.; Bergamaschi, P.; Bousquet, P.; Dlugokencky, E.; Houweling, S.; Ishizawa, M.; Kim, H.S.; Locatelli, R.; Maksyutov, S.; Montzka, S.; Pandey, S.; Patra, P. K.; Pétron, G.; Saunois, M.; Sweeney, C.; Schwietzke, S.; Tans, P.; Weatherhead, E. C. CH_4 emissions from oil and gas production: Have recent large increases been detected? *J. Geophys. Res.-Atmos.*, **2017,** 122, pp. 4070–4083, https://doi.org/10.1002/2016JD026157.
4. IPCC. Summary for Policymakers. In: Climate Change 2021: The Physical Science Basis. Contribution of Working Group I to the Sixth Assessment Report of the Intergovernmental Panel on Climate Change [Masson-Delmotte, V. et al (eds.)]. Cambridge University Press, *IPCC*, Cambridge, United Kingdom and New York, NY, USA, 2021, pp. 3–32, https://doi.org/10.1017/9781009157896.001.
5. Privalova, N.M.; Dvadnenko, M.V.; Nekrasova, A.A.; Privalov, D.M.; Popova, O.S. Impact of oil and oil products on the environment. *Technical Sciences*, **2017**. 10.21515/1990-4665-125-022.
6. Ritchie, H.; Roser, M.; Rosado, P. Greenhouse Gas Emissions". 2020 Published online at OurWorldInData.org. Retrieved from: 'https://ourworldindata.org/co2-and-greenhouse-gas-emissions' [Online Resource].
7. Allen, C.D.; Macalady, A.K.; Chenchouni, H.; Bachelet, D.; McDowell, N.; Vennetier, M.; Kitzberger, T.; Rigling, A.; Breshears, D.D.; Hogg (Ted), E.H.; Gonzalez, P.; Fensham, R.; Zhang, Z.; Castro, J.; Demidova, N.; Lim, J.-H.; Allard, G.; Running, S.W.; Semerci, A.; Cobb, N. A global overview of drought and heat-induced tree mortality reveals emerging climate change risks for forests, *Forest Ecology and Management*, **2010**, 259(4), pp. 660-684.
8. IPCC 2007, *Climate Change 2007: Synthesis Report. Contribution of Working Groups I, II and III to the Fourth Assessment Report of the Intergovernmental Panel on Climate Change* [Core Writing Team, Pachauri, R.K and Reisinger, A. (eds.)]. IPCC, Geneva, Switzerland, 104 pp.
9. Covey, K.R.; Megonigal, J.P. Methane production and emissions in trees and forests. **2019**. *Transley review New Phytologist* pp. 22235-51, doi: 10.1111/nph.15624.
10. Menyailo, O.V.; Abraham, W.-R., Conrad, R. Tree species affect atmospheric CH_4 oxidation without altering community composition of soil methanotrophs. *Soil biology and biochemistry*, **2010**. 42: 101-107.
11. Farquhar, G.D.; Ehleringer, J.R.; Hubick, K.T. Carbon isotope discrimination and photosynthesis Annu. Rev. Plant Phisiol. Plant Mol. Biol.,40, 1989, pp. 503-537.
12. Siegwolf, R.T.W.; Lehmann, M.M.; Goldsmith, G.R.; Churakova (Sidorova), O.V.; Mirande-Ney, C.; Timofeeva, G.; Weigt, R.B.; Saurer, M. Updating dual C and O isotope – Gas exchange model: A concept to understand plant responses to the environment and its implications for tree rings. *Plant, Cell and Environment*, **2023**, pp. 1-22, https://doi.org/10.1111/pce.14630.
13. Farquhar, G.D.; Hubick, K.T.; Condon, A.G.; Richards, R.A. Carbon isotope fractionation and plant water-use efficiency. In: Rundel, P.W., Ehleringer, J.R., Nagy, K.A. **1989** (eds) Stable Isotopes in Ecological Research. Ecological Studies, vol 68. Springer, New York, NY. https://doi.org/10.1007/978-1-4612-3498-2_2.
14. Siegwolf, R.T.W.; Brooks, J.R.; Roden, J. Stable isotopes in tree rings inferring physiological, climatic and environmental responses stable isotope in tree rings. **2022**, p. 773, 10.1007/978-3-030-92698-4.
15. McCarroll, D.; Loader N.J. Stable isotopes in tree rings *Quat. Sci. Rev.*, **2004**, 23: 7–8, pp. 771-801.

16. Quinby, B.M.; Creighton, J.C.; Flacherty, E.A. Stable isotope ecology in insects: a review. Ecological entomology, **2020**, 45, pp. 1231-1246, DOI: 10.1111/een.12934.
17. Guerrieri, R.; Siegwolf, R.T.W.; Saurer, M.; Ripullone, F.; Mencuccini, M.; Borghetti, M. Anthropogenic NOx emissions alter the intrinsic water-use efficiency (WUEi) for *Quercus cerris* stands under Mediterranean climate conditions. Environ Pollut, 2010, 158, pp. 2841–2847.
18. Leonelli G, Battipaglia G, Siegwolf RTW, Saurer M, Morra di Cella U, Cherubini P, Pelfini M (2012) Climatic isotope signals in tree rings masked by air pollution: a case study conductance along the Mont Blanc Tunnel access road (Western Alps, Italy). Atmos Environ 61:169–1719.
19. Romashkino oil field (Ed. R.Kh.Muslimov), v1, VNIIOENG, Moscow, 1995, 492 p.
20. Khasanova, A.; Bakhtina; O. Tatneft estimates reserves of the Romashkinskoye field. 2023. Neftegaz Internet source https://neftegaz.ru/news/gas/774735-tatneft-otsenila-zapasy-romashkinskogo-mestorozhdeniya/.
21. Selley, R.; Sonnenberg, S.A. Elements of Petroleum Geology: Third Edition. 2014. 10.1016/C2010-0-67090-8.
22. Bakin, O.V.; Rogova, T.V.; Sitnikov, A.P. Vascular plants of Tatarstan. University Press. Kazan **2000**, 496 p. https://ourworldindata.org/co2-and-greenhouse-gas-emissions
23. RIHMI-WDC. Baseline Climatological Data Sets. Obninsk, Russia, **2022**. Available online: http:\\meteo.ru\english\data (accessed on 03 December 2022.
24. Cook, E.R.; Kairiukstis, L.A. Methods of dendrochronology. 1990. Applications in the Environmental Sciences, 394 pp. https://doi.org/10.1007/978-94-015-7879-0.
25. Francey, R.J.; Allison, C.E.; Etheridge, D.M.; Trudinger, C.M.; Enting, I.G.; Leuenberger, M.; Langenfelds, R.L.; Michel, E., Steele, E. A 1000-year high precision record of $\delta^{13}C$ in atmospheric CO_2. *Tellus B* 51(2), 1999, pp. 170–193.
26. Rinn, F. TSAPWin – Time series analysis and presentation for dendrochronology and related applications, V. 0.53, User Reference, Heidelberg, 2005.
27. Holmes, R. L. Computer-assisted quality control in tree-ring dating and measurement. Tree-Ring Bulletin, 1983, 43, pp. 51-67.
28. Grissino-Mayer, H.D. Evaluating cross-dating accuracy: A manual and tutorial for the computer program COFECHA. *Tree-Ring Research,* **2001**, 57, pp. 205-221.27.
29. Isodat 2.0 Operating Manual Isodat 2.0 Operating Manual Thermo Electron (Bremen) GmbH. Finnigan Advanced Mass Spectrometry. Bremen, Germany.
30. Saurer, M.; Voelker, S. Intrinsic water-use efficiency derived from stable carbon isotopes of tree rings In *Stable isotopes in tree rings* **2023**, pp. 481-498.
31. Saurer and Siegwolf In Book Stable Isotopes as Indicators of Ecological Change Eds. Todd E. Dawson and Rolf T.W. Siegwolf, **2007**. ISBN: 978-0-12-373627-7.
32. Blackman, R.; Tukey, J.W. The Measurement of Power Spectra from the Point of View of Communications Engineering—Part I. *Bell Syst. Tech. J.* 37, **1958**, pp. 185–282.
33. Khasanova, A.; Bakhtina; O. Tatneft estimates reserves of the Romashkinskoye field. 2023. Neftegaz Internet source https://neftegaz.ru/news/gas/774735-tatneft-otsenila-zapasy-romashkinskogo-mestorozhdeniya/.
34. Pickell, P.D.; Gergel, S.E.; Coops, N.C.; Andison, D.W. Monitoring Forest Change in Landscapes Under-Going Rapid Energy Development: Challenges and New Perspectives. *Land* **2014**, *3*, 617-638. https://doi.org/10.3390/land3030617.
35. Turner, A.J.; Jacon, D.J.; Benmergui, S.C.; Wofsy, J.D.; Maasakkers, A.; Butz, O.; Hasekamp S.C.; Biraud, A. large increase in U.S. methane emissions over the past decade inferred from satellite data and surface observations. *Geophysical Research Letter* 43, pp. 43, 2218–2224, **2016** https://doi.org/10.1002/2016GL067987.
36. Vaganov, E., Hughes, M., Kirdyanov, A. *et al.* Influence of snowfall and melt timing on tree growth in subarctic Eurasia. Nature 400, 149–151, **1999** https://doi.org/10.1038/22087
37. Knorre, A. A., R. T. W. Siegwolf, M. Saurer, O. V. Sidorova, E. A. Vaganov, and A. V. Kirdyanov (2010), Twentiethcentury trends in tree ring stable isotopes (d13C and d18 O) of Larix sibirica under dry conditions in the forest steppe in SiberiaJ. Geophys. Res., 115, G03002, doi:10.1029/2009JG000930.